A Directional Coupler with a Readily Calculable Coupling Ratio

MAURICE B. HALL, MEMBER, IEEE, AND WILLIAM E. LITTLE

Abstract—**A microwave (*X*-band) directional coupler consisting of two adjacent lengths of parallel waveguide with a common tantalum wall about four skin depths in thickness has been fabricated and studied. Coupling between the guides is effected through energy transfer via the electromagnetic fields penetrating the thin tantalum foil separating the guides. The coupling ratio of the device can be calculated by a straightforward procedure to within experimental error (currently a few tenths of a decibel in over 70 decibels).**

I. Introduction

COUPLING coefficients of directional couplers generally can be determined by measurement or by lengthy calculation employing perturbation or variational methods. The holes, slits, etc., through which energy is transferred between the guides, so complicate the field patterns that evanescent higher modes must be included in their formulation.

The precision and reliability of these involved calculations have not yet proved adequate for standards work. Furthermore, the onset of breakdown with increasing power is expected in the vicinity of the holes, etc., where potential gradients are maximum.

A directional coupler consisting of two adjacent parallel rectangular waveguides with a common tantalum wall several skin depths in thickness has been fabricated and studied. Coupling between the guides is effected through energy transfer via the electromagnetic fields penetrating the thin tantalum foil separating the guides. The symmetry of the structure is consistent with the field symmetry of a single transmission mode propagating in each waveguide. Electromagnetic coupling through the thin tantalum separator between "transmission modes" in the two guides can be described theoretically to high accuracy without resorting to the superposition of evanescent higher modes. A simple calculation of the coupling ratio based on the assumption of a pure single mode in each guide and of an RF conductivity within the tantalum common wall equal to the dc conductivity[1] agrees with the measured value to well within the limits of measurement error or of the calculated deviations corresponding to variation in foil thickness. Approximations incident to the calculation (essentially approximations 1) and 5) in Section III) lead to errors that become serious (and increase rapidly with decreasing ratios) at coupling ratios below about 50 dB.[2]

It is expected that the reflection from this type of directional coupler can be reduced, through careful construction, to the minimum possible for a given coupling ratio. The model tested caused a VSWR of between 1.05 and 1.06 for frequencies between 8.2 and 10 GHz.

If adequate foil uniformity can be achieved, the thin-wall coupler will be useful generally in standards work, since the coupling ratio for prescribed foil dimensions can be calculated and then verified. Very high directivity is predicted theoretically. Such a coupler would provide a well-matched fundamental attenuation standard. The coupler, together with a low-power measuring device, would constitute a well-matched feed-through power meter[3] which would possess features particularly desirable in high-power applications. For example, it would strongly reject harmonics and would not lower the breakdown threshold in the high-power channel by introducing electric field distortions. However, the maximum power at which such a coupler is expected to be useful will be limited by conductivity uncertainties arising from heating of the thin wall by the microwave energy.

The device can be adapted to the measurement of bulk RF conductivity within the metal of the thin common wall nearly independently of surface damage or contamination, providing uniform foils of two different thicknesses, but with similar surface conditions, are available.[4]

Manuscript received September 6, 1966; revised June 7, 1967. This work was supported by the Advanced Research Projects Agency under Project DEFENDER, ARPA 515, and was monitored by M. I. Witow.

M. B. Hall is with the Radio Standards Lab., National Bureau of Standards, Boulder, Colo. 80302.

W. E. Little was formerly with the Radio Standards Lab., National Bureau of Standards. He is currently with the Space Disturbance Lab., Institute of Telecommunication Sciences and Aeronomy, Boulder, Colo. 80302

[1] The dc conductivity, measured parallel to the surfaces, of the tantalum foil used was within 2 percent of the published value for the bulk conductivity (Table I page 603). Incident power levels were below 75 mW.

[2] As used in this paper, coupling ratios are given in decibels by

$$10 \log_{10} \frac{\text{level of supplied power}}{\text{level of coupled power}}.$$

[3] G. F. Engen, "A variable impedance power meter, and adjustable reflection coefficient standard," *Engrg. and Instrum. J. Research NBS*, vol. 68C, no. 1, January–March 1964.

[4] If uniform conductivity within the thin metal common wall is assumed, the coupling ratio in decibels for a given material can be expressed as a sum of two terms, a constant term (with respect to thickness) determined by boundary conditions at the foil surfaces and a term deriving from the attenuation in the metal. In the calculation of bulk conductivity from coupling ratio data on actual foils, possible errors resulting from conductivity deviations within surface layers very thin with respect to the foil thickness can be circumvented essentially by inserting σ, the bulk conductivity, in the thickness dependent term and assuming thickness independence of the attenuation through the interfaces and thin surface layers within which the conductivity varies. Then, by measuring the coupling ratio for two foil thicknesses, one can eliminate the thickness-independent term and with it the need to consider deviations of conductivity at the surface, and relate the difference in coupling ratio to the bulk value of the conductivity.

II. Description of Coupler

Essentials of the directional coupler which has been examined at the Boulder Labs.[5] are shown in the cross-sectional diagrams of Fig. 1. A tantalum foil 300 ± 10 microinches in thickness is clamped between two brass blocks into which the two waveguide channels are machined. Closely spaced (about every 0.5 inch) quarter-inch bolts draw the blocks together into a rigid structure with the taut foil supported between the blocks.

Leakage from the structure could not be detected with a search probe (i.e., horn) sensitive to a level 100 dB below the maximum level within the coupler. Such a degree of leakage suppression is consistent with prior experience with this construction technique.

The machined channels are 0.9 inch wide by 0.4 inch high, coinciding with the internal dimensions of standard WR 90 rectangular waveguide. The structure depicted in Fig. 1 thus constitutes two waveguides separated along the parallel portion by the tantalum foil only. The tantalum foil constitutes one 0.9 inch wide boundary of each guide. Power enters port 1, and most of it emerges from port 2. A minute amount penetrates the tantalum wall and, in general, emerges from ports 3 and 4. The thin tantalum foil "window," in one of the two models that were built and tested, is three wavelengths long; in the other, it is six wavelengths long. In these cases, and in general when the length of the window is an integral number of half wavelengths long, very nearly all of the minute amount of energy penetrating the window emerges from port 4. Wave components which individually would leave port 3 via successive increments of window length as a result of excitation by a wave incident at port 1 are mutually eliminated by destructive interference.

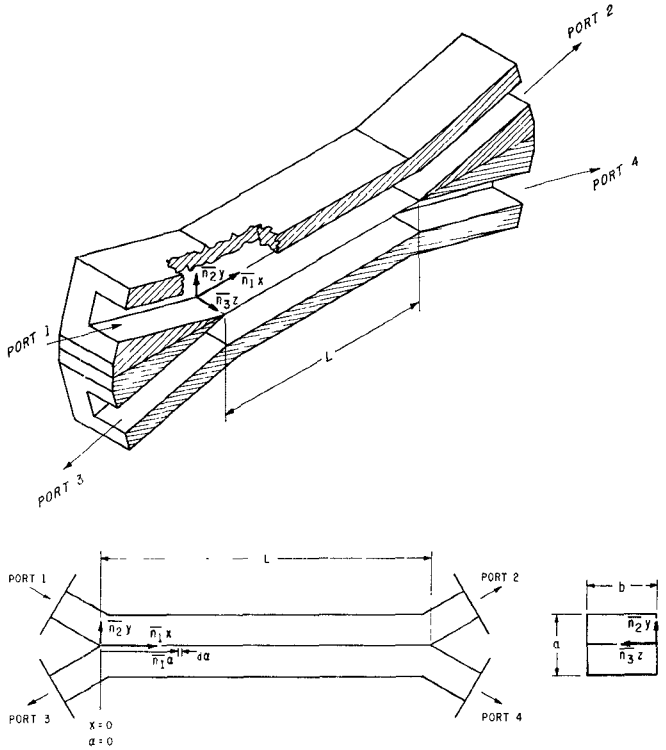

Fig. 1. Thin-wall directional coupler.

In what is to follow, field distortions, due to the presence of the 15 degree bends at $x=0$ and $x=L$ in the guides of Fig. 1, will be ignored without justification because in a contemplated design the bends will be less abrupt and will be removed from the proximity of the thin common wall. A published[6] theoretical analysis of mitered waveguide corners predicts a reflection coefficient modulus of 0.08 for the 15 degree bends at the design frequency (9 GHz) of the device of Fig. 1. The design improvements will be facilitated by soldering the thin tantalum common wall within an all-tantalum structure. The device of Fig. 1 provided some flexibility considered desirable for initial tests. It yielded data in agreement with calculated results to well within the limits of measurement error.

III. Determination of Coupling Ratio

The field within the metal of the thin wall constituting the coupling window can be calculated by an extension of the method used by Jackson[7] to calculate the dissipation from an electromagnetic field in an imperfectly conducting bounding medium. The fields penetrating the medium are subject to Maxwell's equations and to the further condition that the magnetic field component parallel to the air-metal interfaces must be continuous across the interfaces. Assume a wave of a frequency which WR 90 (X-band) waveguide will transmit in a single mode only to be incident on port 1 of the device of Fig. 1 and assume the absence of incident waves at the other ports. The magnetic field in this upper section of guide will have only components parallel to, and the electric field will have only a component perpendicular to, the window surface. The subsequent analysis is referred to a right-hand coordinate system with the origin in the upper surface of the thin metal window as shown in Fig. 1.

In this coordinate system and in rationalized MKS units (to be used throughout this paper), the magnetic field in the upper section of waveguide is expressible as [8]

$$H_1 = \left(-n_1 \cos\frac{\pi}{b} z - n_3 j\beta \frac{b}{\pi} \sin\frac{\pi}{b} z\right) B e^{j(\omega t - \beta x)} \quad (1a)$$

and the electric field as

$$E_1 = \left(-n_2 j\omega\mu_0 \frac{b}{\pi} \sin\frac{\pi}{b} z\right) B e^{j(\omega t - \beta x)}. \quad (1b)$$

[5] It has come to our attention that a study of a resistance strip coupler was conducted by M. S. Tanenbaum, Polytechnic Institute of Brooklyn, Brooklyn, N. Y., M.S. thesis, Rept. R-225-49, PIB-170. However, Tanenbaum's device and analysis differ basically from those of this paper. Thus, the coupling element in Tanenbaum's coupler was a resistance strip consisting of a platinum-coated glass plate and situated in an opening in a common wall between two adjacent guides. His analysis was based on a lumped constant approach.

[6] N. Marcuvitz, *Waveguide Handbook*. New York: McGraw-Hill, 1951, pp. 316–317.

[7] J. D. Jackson, *Classical Electrodynamics*. New York: Wiley, 1962, pp. 236–240.

[8] S. Flugge, Ed. "Electric fields and waves" in *Encyclopedia of Physics*, vol. 16. Berlin, Germany: Springer, 1958, p. 317.

Here H_1 and E_1, respectively, are the magnetic and electric field vectors in the upper waveguide; n_1, n_2, and n_3 are unit vectors as shown in Fig. 1; B is the amplitude of the magnetic field parallel to the direction of propagation; b is the width of the guide (i.e., the inside dimension in the n_3 direction, Fig. 1); μ_0 is the permeability of the medium filling the guide; and β is equal to $2\pi/\lambda$, where λ is the guide wavelength of the TE_{10} mode.

These expressions are seen to be independent of y, that is, the magnetic and electric field vectors do not vary with position along the direction of the electric vector. Equation (1a) then gives the magnetic field generated in the upper guide adjacent and parallel to the upper surface of the metal window by the TE_{10} wave passing through the upper waveguide from port 1 to port 2. It is assumed that:

1) The amplitude of the wave through the upper guide is constant with respect to x; that is, the wave is not attenuated by dissipation in the guide walls or by leakage out of the guide through the metal window. This assumption implies a limitation on L and on the coupling ratio and eliminates the need to consider coupling from the lower back to the upper guide.

2) Because of the high conductivity of the metal, only normal electric and tangential magnetic fields exist (in our case the fields of the TE_{10} rectangular waveguide mode) adjacent to the metal surface, as would be rigorously true only if the surface were infinitely conducting.

3) Within the metal window, the comparatively very slow variations of the field components with distance parallel to the window surface are zero with respect to the variations perpendicular to the surface; and hence, within the metal the operator curl can be written $-n_2\,\partial/\partial\,\xi$, where n_2, as defined previously, is the unit vector upward from and perpendicular to the surface of the metal window and where ξ is a variable which increases positively with distance into the metal from the top surface along a coordinate axis perpendicular to the metal window surface (i.e., ξ is equal to $-y$). This assumption is valid because of the very rapid attenuation of the fields in the metal.

4) The displacement current is negligible with respect to the conduction current within the metal foil.

5) The thickness of the foil is sufficient to isolate the surfaces, sufficient, that is, to justify neglecting the amplitude within the metal foil at the top air–metal interface of the wave reflected from the bottom metal–air interface.

Assumption 5) reduces the calculation of the wave downward through the metal foil to a calculation of the wave that would be excited by the fields in the upper guide in a bounding metal medium of infinite thickness. Subject to the simplifications introduced by approximations 1) to 5), the solution for the region within the metal wall (assumed infinitely thick) of Maxwell's equations which provides for continuity of the parallel (to the interface) component of the magnetic vector at the top interface is[7]

$$H_c(i) = H_1 e^{-\xi(1+j)/\delta}$$

$$E_c(i) = \sqrt{\frac{\mu_c\omega}{2\sigma}}\,(1+j)(n_2 \times H_1)e^{-\xi(1+j)/\delta}. \tag{2}$$

Here, δ the skin depth in the metal is given by

$$\delta = \sqrt{\frac{2}{\mu_c\sigma\omega}} \tag{3}$$

in terms of the permeability μ_c and conductivity σ of the metal window medium. H_1 is given by (1a).[9] The wave excited by the fields in the upper waveguide propagates through the metal foil from the upper to the lower air-metal interface in the direction perpendicular to the interfaces. The electric vector $E_c(i)$ and magnetic vector $H_c(i)$ of this wave are obtained in terms of measurable quantities by combining (1) and (2).

At the lower face of the metal window, i.e., the face constituting the upper wall of the lower waveguide, a portion of the energy in this incident wave is reflected. The fraction of energy reflected at any point on the interface is determinable from a) the knowledge that the time average of the total energy crossing the interface into the lower guide must equal the time average energy emerging from ports 3 and 4 of the lower guide, and b) the knowledge that the component of the magnetic field vector tangential to the metal window must be continuous across the boundary. Pursuant to calculating this reflected energy, we write the magnetic $H_c(r)$ and electric $E_c(r)$ field vectors of the wave reflected from the interface between the metal window and lower guide as follows:

$$H_c(r) = -\bar{\Gamma}_0 \cdot H_1 e^{\xi(1+j)/\delta}$$

$$E_c(r) = \sqrt{\frac{\mu_c\omega}{2\sigma}}\,(1+j)[n_2 \times (\bar{\Gamma}_0 \cdot H_1)]e^{\xi(1+j)/\delta}. \tag{4}$$

To provide for variation of reflected amplitude with polarization as well as position, we have represented by the dyadic, $\bar{\Gamma}_0 = {}^x\Gamma_0\, n_1 n_1 + {}^z\Gamma_0 n_3 n_3$, the reflection coefficient (complex) within the metal window at its upper surface; i.e., in the limit $\xi \to 0$. Here ${}^x\Gamma_0$ and ${}^z\Gamma_0$ are reflection coefficients (for $\xi \to 0$) as ordinarily written for waves with magnetic vectors parallel to the $\xi - x$ and $\xi - z$ planes, respectively. The magnitudes in $\bar{\Gamma}_0$ are very small, less than 0.0005, since they are the fractions of the amplitude components remaining after two traversals of the metal window. This is the basis of assumption 5).

Utilizing Poynting's theorem, we may write the time-average energy flow P_c across a plane section of the metal window a distance ξ below and parallel to its interface with the upper waveguide

[9] For foils of thinness sufficient to invalidate approximation 5) of Section III, one would set H_1 of (1b) equal to H_c of (6) at the boundary between the upper guide and the metal window ($\xi = 0$) instead of neglecting $H_c(r)$ as is done here.

$$P_c = \int_0^L \int_0^b -\frac{1}{2} \operatorname{Re}\,(\boldsymbol{n}_2 \cdot \boldsymbol{E}_c \times \boldsymbol{H}_c^*) dxdz \tag{5}$$

where $\boldsymbol{E}_c$ and $\boldsymbol{H}_c$ respectively, are the resultants of electric and magnetic field components within the metal, L is the linear dimension of the window in the $\boldsymbol{n}_1$ direction, and the other symbols are as previously defined. For $\xi = d$, the window thickness P_c becomes the energy emerging through the window into the lower guide.

Now in terms of the components defined in (2) and (4),

$$\begin{aligned} \boldsymbol{E}_c &= \boldsymbol{E}_c(i) + \boldsymbol{E}_c(r) \\ \boldsymbol{H}_c &= \boldsymbol{H}_c(i) + \boldsymbol{H}_c(r). \end{aligned} \tag{6}$$

Combination of (1), (2) and (4) through (6) leads to[10]

$$\begin{aligned} P_c = \int_0^L \int_0^b \frac{1}{2} \sqrt{\frac{\mu_c \omega}{2\sigma}}\, B^2 e^{-2\xi/\delta} \\ \cdot \left[(1 - |{}^x\Gamma|^2 - 2|{}^x\Gamma| \sin {}^x\gamma) \cos^2 \frac{\pi}{b} z \right. \\ \left. + (1 - |{}^z\Gamma|^2 - 2|{}^z\Gamma| \sin {}^z\gamma) \beta^2 \frac{b^2}{\pi^2} \sin^2 \frac{\pi}{b} z \right] dxdz \end{aligned} \tag{7}$$

where

$$\begin{aligned} {}^x\Gamma &= |{}^x\Gamma|\, e^{j {}^x\gamma} = {}^x\Gamma_0 e^{2\xi(1+j)/\delta}, \\ {}^z\Gamma &= |{}^z\Gamma|\, e^{j {}^z\gamma} = {}^z\Gamma_0 e^{2\xi(1+j)/\delta}. \end{aligned} \tag{8}$$

At the interface between the metal window and lower waveguide, ξ, $|{}^x\Gamma|$, $|{}^z\Gamma|$, ${}^x\gamma$, ${}^z\gamma$, and P_c become, respectively, d, $|{}^x\Gamma_d|$, $|{}^z\Gamma_d|$, ${}^x\gamma_d$, ${}^z\gamma_d$, and P_d. The value P_d is then the power flow into the lower guide.

The knowledge that the tangential component of the magnetic field vector must be continuous across the interface permits, if certain reasonable assumptions are made, the replacement in (7) of $|{}^x\Gamma|^2$, $|{}^z\Gamma|^2$, $2|{}^x\Gamma| \sin {}^x\gamma$, and $2|{}^z\Gamma| \sin {}^z\gamma$ by known functions of the power leaving the lower guide. A basic assumption is: since the symmetries of both waveguides are consistent with a simple TE_{10} mode, the fields in the lower guide are the sums of TE_{10} components only. This assumption neglects second-order fields which arise as a result of finite wall conductivity.

The magnetic field at any plane perpendicular to the propagation direction in the lower waveguide is invariant with y and may be considered to be constituted of interfering TE_{10} wavelets, one wavelet arriving at the point via each increment of window length. It is convenient to integrate the expression representing wavelets arriving at any plane into two terms, one representing the resultant wave propagating toward the left and the other representing the resultant wave propagating toward the right. The field at any plane is then the sum of these two terms and may be set equal to $\boldsymbol{H}_c$ (for $\xi = d$) of (6). The resulting equations may then be solved for $|{}^x\Gamma_d|^2$, $|{}^z\Gamma_d|^2$, $2|{}^x\Gamma_d| \sin {}^x\gamma_d$, and $2|{}^z\Gamma_d| \sin {}^z\gamma_d$ which are required for substitution into (7).

The wavelets constituting the term representing the wave propagating in the positive x direction in the lower guide will be integrated first. Recall that the assigned $x = 0$ plane of Fig. 1 intersects the left extreme of the metal window of length L; that is, the metal window extends from $x = 0$ to $x = L$. The magnetic field incident on the interface between the metal window and lower waveguide is, according to (1) and (2)

$$\begin{aligned} &\boldsymbol{H}_c(i) \\ &= \left[\left(-\boldsymbol{n}_1 \cos \frac{\pi}{b} z - \boldsymbol{n}_3 j\beta \frac{b}{\pi} \sin \frac{\pi}{b} z \right) B e^{j\omega t} e^{-d(1+j)/\delta} \right] e^{-j\beta x} \end{aligned}$$

where d equals $\xi_{\max}$, the tantalum foil thickness. Hence, the magnetic field $\overrightarrow{d\boldsymbol{H}_2}$ of the wavelet in the $\boldsymbol{n}_1$ direction in the lower guide arriving at the position x, via the element of window length $d\alpha$, may be considered conveniently (for a reason which will become apparent) as the sum of a component excited by, and proportional at $x = \alpha$ to, the $\boldsymbol{n}_1$ component of $\boldsymbol{H}_c(i)$ and a component excited by, and proportional at $x = \alpha$ to, the $\boldsymbol{n}_3$ component of $\boldsymbol{H}_c(i)$. Accordingly, we may write

$$\begin{aligned} \overrightarrow{d\boldsymbol{H}_2} = (U + V) d\alpha \left(-\boldsymbol{n}_1 \cos \frac{\pi}{b} z - \boldsymbol{n}_3 j\beta \frac{b}{\pi} \sin \frac{\pi}{b} z \right) B e^{j\omega t} \\ \cdot e^{-d(1+j)/\delta} e^{-j\beta x} \end{aligned} \tag{9}$$

where U and V are complex constants of proportionality. Here, on identical coordinate axes, x denotes the position at which the magnetic field is observed and α the position of the window element through which the wavelet under consideration emerges into the lower guide.

The term representing the magnetic vector of the wave propagating in the positive x direction is, at the plane x, given by the sum of the components, $\overrightarrow{d\boldsymbol{H}}$, contributed by the wavelets represented by (9); thus

$$\begin{aligned} \overrightarrow{\boldsymbol{H}_2} = \int_{\alpha=0}^{\alpha=x} \overrightarrow{d\boldsymbol{H}_2} = \int_{\alpha=0}^{\alpha=x} (U + V) \left(-\boldsymbol{n}_1 \cos \frac{\pi}{b} z \right. \\ \left. - \boldsymbol{n}_3 j\beta \frac{b}{\pi} \sin \frac{\pi}{b} z \right) B e^{j(\omega t - \beta x)} e^{-d(1+j)/\delta} d\alpha. \end{aligned} \tag{10}$$

Similarly, the term representing the magnetic vector of the wave propagating in the negative x direction is, at the plane x, given by the sum of the components $\overleftarrow{d\boldsymbol{H}}$ contributed by the wavelets emerging into the lower guide through increments of α to the right of the plane x; thus

$$\begin{aligned} \overleftarrow{\boldsymbol{H}_2} = \int_{\alpha=x}^{\alpha=L} (U - V) \left(-\boldsymbol{n}_1 \cos \frac{\pi}{b} z \right. \\ \left. + \boldsymbol{n}_3 j\beta \frac{b}{\pi} \sin \frac{\pi}{b} z \right) B e^{j(\omega t + \beta x)} e^{-d(1+j)/\delta} e^{-j2\beta\alpha} d\alpha. \end{aligned} \tag{11}$$

[10] The meaning of the terms $2|{}^x\Gamma| \sin {}^x\gamma$ and $2|{}^z\Gamma| \sin {}^z\gamma$ is discussed in G. Persky, "The sinusoidal variation of dissipation along uniform waveguides," *IRE Trans. Microwave Theory and Techniques*, vol. MTT-10, pp. 592–595, November 1962.

The total magnetic flux density, i.e., magnetic field, in the lower guide at the plane x is then

$$\begin{aligned}\boldsymbol{H}_2 &= \overrightarrow{\boldsymbol{H}}_2 + \overleftarrow{\boldsymbol{H}}_2 \\ &= \Big[(U+V)\Big(-\boldsymbol{n}_1\cos\frac{\pi}{b}z - \boldsymbol{n}_3 j\beta\frac{b}{\pi}\sin\frac{\pi}{b}z\Big)x \\ &\quad + j\frac{1}{2\beta}(U-V)\Big(-\boldsymbol{n}_1\cos\frac{\pi}{b}z + \boldsymbol{n}_3 j\beta\frac{b}{\pi}\sin\frac{\pi}{b}z\Big) \\ &\quad \cdot (e^{-j2\beta(L-x)} - 1)\Big] Be^{j(\omega t-\beta x)}e^{-d(1+j)/\delta}. \qquad (12)\end{aligned}$$

For $x=0$ and $L=n\lambda/2$, where n is an integer, $\overleftarrow{\boldsymbol{H}}_2$ and $\boldsymbol{H}_2$ are equal to zero. Hence, for maximum directivity, L has been made an integral number of half wavelengths in the models that have been studied. For $x \geqq L$, the magnetic field in the lower guide may be written

$$\boldsymbol{H}_2 = Ge^{j\theta}\Big[-\boldsymbol{n}_1\cos\frac{\pi}{b}z - \boldsymbol{n}_3 j\beta\frac{b}{\pi}\sin\frac{\pi}{b}z\Big]e^{j(\omega t-\beta x)} \qquad (13)$$

where G is the constant amplitude of the $\boldsymbol{n}_1$ component and θ is a constant such that $\beta x+\theta$ is the phase of $\boldsymbol{H}_2$ relative to that of the wave at $x=0$ in the upper guide. At $x=L$, if $U+V=|U+V|e^{j\phi}$, (12) and (13) yield

$$\begin{aligned}|U+V| &= \frac{G}{LBe^{-d/\delta}}, \\ \theta &= \phi - \frac{d}{\delta}. \qquad (14)\end{aligned}$$

The resultant magnetic field within the metal window adjacent to its interface with the lower guide is tangential to the interface, and given by the value of (6) at the interface, i.e., the value of (6) for $\xi=d$. The magnetic field vector in the lower guide tangential to the surface of the metal window is given by $\boldsymbol{H}_2$ of (12). Since the tangential magnetic field component is continuous across the interface between the metal window and lower guide, we may equate $\boldsymbol{H}_2$, as given by (12), to $\boldsymbol{H}_c$ for $\xi=d$, as given by (2), (4), and (6). The $\boldsymbol{n}_1$ and $\boldsymbol{n}_3$ components of this equation yield, respectively,

$$\begin{aligned}{}^x\Gamma_d &= |{}^x\Gamma_d|e^{j{}^x\gamma_d} \\ &= 1 - (U+V)x - j\frac{1}{2\beta}(U-V)(e^{-j2\beta(L-x)} - 1)\end{aligned}$$

and

$$\begin{aligned}{}^z\Gamma_d &= |{}^z\Gamma_d|e^{j{}^z\gamma_d} \\ &= 1 - (U+V)x + j\frac{1}{2\beta}(U-V)(e^{-j2\beta(L-x)} - 1). \qquad (15)\end{aligned}$$

Equations (14) and (15) permit the substitution of measurable or negligible quantities for $|{}^x\Gamma_d|$, $|{}^z\Gamma_d|$, ${}^x\gamma_d$, and ${}^z\gamma_d$ in (7). Substitution from (15) into (7) and subsequent integration lead after discarding of negligible (less than 0.01 percent) terms to

$$\begin{aligned}P_d = \frac{b}{4}\sqrt{\frac{\mu_c\omega}{2\sigma}}B^2e^{-2d/\delta}\Big[\Big(|U+V|L^2(\cos\phi+\sin\phi) \\ - |U+V|^2\frac{L^3}{3}\Big)\Big(1+\beta^2\frac{b^2}{\pi^2}\Big) \\ + \Big(\frac{|U-V|L}{\beta}(\sin\psi-\cos\psi)\Big) \\ \cdot\Big(1-\beta^2\frac{b^2}{\pi^2}\Big)\Big]. \qquad (16)\end{aligned}$$

The energy emerging from port 4 may be written[11]

$$P_4 = \frac{b^2}{4\pi^2}\omega\mu_0\beta abG^2. \qquad (17)$$

For $L=n\lambda/2$, $P_4=P_d$, whence, if the last term of (16) is neglected at a cost of less than 0.3 percent error and if $|U+V|$ is substituted from (14):

$$\frac{G}{B} = \frac{(\pi^2+\beta^2b^2)(\cos\phi+\sin\phi)Le^{-d/\delta}}{\sqrt{\frac{2\sigma\mu_0{}^2\omega}{\mu_c}}\beta ab^2 + \frac{L(\pi^2+\beta^2b^2)}{3}}. \qquad (18)$$

Now, ϕ is related to measurable quantities by (14). The measurements tabulated below lead to $d/\delta=3.829$ radians. Relative to the phase of the wave through the upper guide at $x=0$, $\beta x+\theta$ is the phase of the wave in the lower guide and βx is the phase of the wave in the upper guide for values of x greater than L. The phase of the wave emerging from port four then lags that of the wave from port 2 by the angle θ, since, after passing $x=L$ at which θ is defined, the two waves traverse equal paths and experience similar distortions.

This phase lag was measured using the coupler with the 6-wavelength long window and a phase measurement system described in the literature.[12] θ was found to be -178.65 ± 2.3 degrees $= -3.118 \pm 0.04$ radians. Substitution of $\theta=-3.118$ radians and $d/\delta=3.829$ radians into (14) yields $\phi=0.711$ radians $=40.73$ degrees. Because of the high attenuation from port 1 to port 4 through the directional coupler, the accuracy of this phase measurement was lower than would have been possible with a more intense source. A several degree error in ξ/δ is possible. However, higher accuracy is unnecessary for present purposes. Thus, if in (18) ϕ were set equal to 45 instead of 40.73 degrees, an error of less than $\frac{1}{3}$ percent would occur in the term embodying $\cos\phi+\sin\phi$.

[11] G. C. Southworth, *Principles and Applications of Waveguide Transmission*. New York: Van Nostrand, September 1961, p. 104.

[12] D. A. Ellerbruch, "Evaluation of a microwave phase measurement system," *Engrg. and Instrum., J. Research NBS*, vol. 69C, no. 1, January–March 1965.

TABLE I

PERTINENT COUPLING WINDOW MEASUREMENTS

Symbol	Quantity	Source or Derivation	Numerical Value in MKS Units	
σ	conductivity of tantalum foil	measured	$7.10 \pm 0.01(10)^6$	mhos/meter
		from table*	$7.24\ (10)^6$	mhos/meter
d	thickness of tantalum foil	measured	$7.62 \pm 0.25(10)^{-6}$	meters
L (for coupler #1)	length of window	measured	0.1461 ± 0.00013	meters
L (for coupler #2)	length of window	measured	0.2921 ± 0.00013	meters
δ	skin depth in tantalum foil	$\delta = \sqrt{2/\mu_c \omega \sigma}$	$1.99(10)^{-6}$	meters
d/δ	foil thickness in skin depths		3.829	

* *American Institute of Physics Handbook.* New York: McGraw-Hill, p. 273.

Five thousandths of an inch is a very conservative upper limit to the measured difference in the lengths of guide between the edge of the metal window ($X=L$) and the planes of the flange faces to which the phase-difference measurement was referred. At 9 GHz, the frequency at which tests were conducted, the length difference corresponds to a phase error of about 1 degree and an error in the coupling ratio of a little over 0.1 percent.

The dc resistivity of the foil parallel to the surfaces was determined from the measured resistance between two brass clamps supporting between them a square area of the foil. The measured value was within 2 percent of the published value for the bulk conductivity.

The coupling ratios of two directional couplers were measured. The couplers differed only in that the length of window L in one was twice that in the other. In accordance with (18), the measured difference in coupling ratios was 6 dB to within the limits of accuracy of the measurements.

Table I lists the various measured quantities and readily derived quantities appearing in (18). The column headings are self explanatory.

The coupling ratio computed from (18) for the coupler with the 0.2921 meter long window, using the measured value of ϕ (40.73 degrees) and the nominal window thickness (300 microinches) is 72.3 dB. The measured value was 72.2 dB. The extremes of measured thickness values, i.e., 290 and 310 microinches, correspond to computed coupling ratios of about 71.25 and 73.39 dB for the coupler with the six wavelength long window. The possible error in the coupling ratio measurement was several tenths of a decibel.

For each coupler, the measured directivity exceeded 30 decibels, the maximum directivity that could be distinguished with the equipment with which the measurements were made.

ACKNOWLEDGMENT

The authors are indebted to B. J. Kinder for the coupling ratio and directivity measurements, D. A. Ellerbruch for the phase measurements, and to J. R. M. Vaughan of General Electric Company for pointing out that the coupler, as a component of a feed-through power meter, would discriminate against harmonics.